

# Krypton fluoride excimer laser for advanced microlithography

Uday K. Sengupta

Cymer Laser Technologies, Inc.  
16275 Technology Drive  
San Diego, California 92127-1815

**Abstract.** The excimer-laser-based stepper is now expected to play a significant role in the manufacturing of ULSI devices requiring sub-0.4- $\mu\text{m}$  design rule features. They will be used in a mix-and-match strategy along with high NA *i*-line steppers for critical layers in the production of 64-Mbit dynamic random access memory (DRAM) generation of IC devices. This is supported by the present availability of a number of production worthy high-NA, wide-field excimer stepper models, along with the recent introduction of several process worthy and moderate cost, positive tone deep-UV photoresists. The excimer laser for the stepper, since its introduction in 1987, has evolved from a laboratory instrument to fully production worthy fab-line equipment. The status of such a laser is discussed. We will discuss the operating theory and the design features of an excimer laser; in particular, the discharge chamber, spectral narrowing module, and the wavemeter. Some of the latest technical innovations incorporated into the laser that reduce maintenance intervals and increase reliability are also presented. Finally we will present and discuss the performance specifications of a current production lithography excimer laser.

*Subject terms:* microlithography; excimer laser-based stepper; deep-UV lithography.

*Optical Engineering* 32(10), 2410–2420 (October 1993).

## 1 Introduction and Background

Microlithography for advanced ULSI fabrication is now making a transition from *i*-line (365 nm) to deep-UV (248 nm); namely, from a mercury arc lamp to an excimer laser as the illumination source. The excimer-laser-based stepper is, therefore, expected to become one of the primary lithography tools for printing sub-0.4- $\mu\text{m}$  design rule features. It will be used in a mix-and-match strategy along with high-NA *i*-line steppers for some critical layers in the production of 64-Mbit dynamic random access memory (DRAM) generation of devices.<sup>1</sup> This is also supported by the current availability of a number of production worthy high-NA, wide-field excimer stepper models,<sup>2,3</sup> along with the recent introduction of several process worthy, moderate cost, positive-tone deep-UV photoresists.<sup>4,5</sup>

Although the *i*-line process with special “enhancements,” such as the use of phase-shift masks or oblique illumination is able to achieve sub-0.4- $\mu\text{m}$  resolution, it has severe limitations. These include the inability to print generalized features, problems with phase-shift-mask inspection and repair,

complex circuit design layout, lack of flexibility, decrease in throughput, and limited process latitude.<sup>6</sup> Decreasing the wavelength, on the other hand, provides one with the simplest and the most cost effective means to improve resolution.

Does the transition from *i*-line to the excimer laser pose major challenges? For the stepper and laser makers, yes; but all issues have now been solved. For the photoresist manufacturer, possibly; but it is an issue of new chemistry at shorter wavelengths and not the laser. However, good resists are now available. However, for the IC maker, the introduction of the excimer laser will be almost transparent. They will experience higher equipment availability at comparable or lower stepper operating costs. Resist processing complexity may still be an issue. Nevertheless, deep-UV lithography is becoming viable and process worthy rapidly.

Advanced lithography tools fall into two categories: (1) an all refractive lens reduction stepper or (2) a catadioptric scanning imaging system. The first one uses an all refractive reduction lens ( $\times 4$  or  $\times 5$ ) to directly image the reticle pattern on the wafer. The second exposure system uses a reflective reduction ( $\times 4$ ) imaging system with some refractive optics. This system is based on imaging the reticle pattern on the wafer by scanning a slit exposure source across the reticle. As is discussed later, for an illumination source

Paper MIC-06 received Mar. 31, 1993; revised manuscript received May 11, 1993; accepted for publication May 15, 1993.  
© 1993 Society of Photo-Optical Instrumentation Engineers. 0091-3286/93/\$6.00.

**Table 1** Stepper performance and required laser specification.

STEPPER	1st (1988/89)	2nd (1990/92)	3rd (1993/94)
NA	0.35	0.4 - 0.45	0.35 - 0.53 (variable)
Field Size (mm)	21 Ø	21 Ø, 25 Ø	> 30 Ø
Optical throughput Efficiency	5 - 8%	≥ 10%	≥ 15%
<b>LASER</b>			
Spectral bandwidth:			
FWHM (pm)	≤ 3	≤ 2.2	≤ 1.3
95% Energy Band (pm)	---	< 7	< 4
Center Wavelength Stability (pm)	≤ ± 1	≤ ± 0.5	≤ 0.25
Pulse Energy Variation (σ)	≤ 3.5%	≤ 3 %	≤ 2.5 %
Power	2-3W	4W	6W
Repetition Rate (Hz)	200	400	500

whose wavelength is below 300 nm, the stepper needs a spectrally narrowed ( $\Delta\lambda < 2$  to 3 pm) light source, whereas the step-and-scan tool uses a broadband source ( $\Delta\lambda \sim 3$  to 4 nm). In both cases, a laser source at 248 nm can be used. This paper primarily discusses the spectrally narrowed KrF excimer laser for the stepper. However, it is simply a subset of the broadband laser. There are four major suppliers of deep-UV steppers today, Canon, Nikon, GCA, and ASM-L, whereas only SVG-L manufactures a deep-UV step-and-scan lithography tool. Deep-UV (less than 300 nm) steppers use an excimer laser; the step-and-scan system, on the other hand, presently employs a deep-UV enhanced mercury lamp. Both lithography system types are expected to use a 193 nm (argon fluoride) excimer laser for their next generation (sub-0.25- $\mu\text{m}$  features) tool.

Incidentally, the excimer laser is almost an ideal illumination source for lithography. The output is spatially incoherent (coherence length approximately 100 to 200  $\mu\text{m}$ ) like a lamp, but is spectrally narrow compared to a lamp, which allows for a simpler optic and illuminator design. The laser is efficient, 0.6% for a spectrally narrowed and greater than 2% for a broadband laser. It is able to provide precise illumination on command, with no decrease in output power (therefore, no loss in throughput, as is the case with a mercury lamp near the end of its life). The laser is also suited for implementing enhanced illumination schemes, such as quadrupole or annular, with minimal loss of throughput. The laser can be installed remotely, which eliminates any unnecessary thermal loading on the stepper or the enclosure. Finally, the laser operating cost is now comparable to the cost of exchanging mercury lamps in advanced production lithography tools.

As is well known, below 300 nm there is only one suitable optical material available for building the stepper lens—fused silica. Other materials, such as  $\text{CaF}_2$ ,  $\text{MgF}_2$ , or  $\text{LiF}$ , although transparent in deep UV are unsuitable because they are crystalline, birefringent, and have high thermal expansion coefficients. An all fused silica stepper lens, as a result, will have no chromatic correction capability. Therefore, the spectral bandwidth of the illumination source has to be reduced and the required bandwidth is a function of the lens numerical aperture (NA). A mercury lamp using filters is incapable of this task; only an optical amplifying medium such as a spec-

**Table 2** Laser parameters versus stepper performance.

Spectral Bandwidth and Spectral Energy Distribution	⇒	Resolution, Depth of Focus
Relative Wavelength Stability	⇒	Focal Plane Stability (long term) Resolution, D.O.F., (Short Term)
Absolute Wavelength Stability	⇒	Magnification, Distortion
Output Power	⇒	Throughput
Repetition Rate	⇒	Energy Dose Accuracy, Speckle Reduction
Pulse-to-Pulse Energy Stability	⇒	Energy Dose Accuracy
Beam Profile, Beam Pointing & Beam Divergence Stability	⇒	Exposure Uniformity, Illuminator Efficiency
Polarization Stability	⇒	Illuminator Efficiency
Spatial Coherence	⇒	Speckle, Exposure Uniformity

⇒ implies affects

trally narrowed excimer laser will be able to meet all the necessary requirements. Table 1 presents both the stepper performance and the corresponding required laser specifications over three generations of excimer stepper models.

To better understand the excimer stepper and the lithography process, it is helpful to establish some simple relationships between laser parameters and corresponding stepper performance. This is done in Table 2, which is self-explanatory and shows a multifaceted relationship between the laser and the stepper. Such is not the case with the mercury arc lamp and the stepper.

In the next section, we discuss the theory, design, and performance of an excimer laser for lithography. All excimer stepper makers today use a common laser, from one laser manufacturer; this paper therefore focuses primarily on the performance and design of this laser.<sup>7</sup> The basic operating principles of all lithography lasers are, however, similar.

## 2 Lithography Excimer Laser

The term “excimer” comes from “excited dimer,” a class of molecules that exists only in the upper excited state but

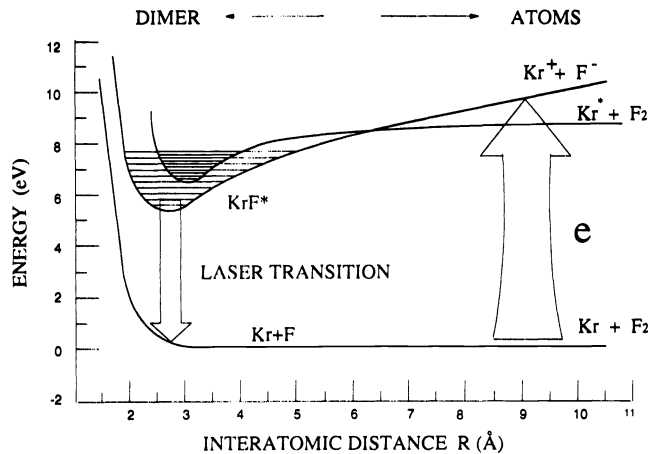


**Fig. 1** Energy diagram for a  $\text{KrF}^*$  excimer laser.  $\text{KrF}^*$  is formed via two reaction channels. It decays to the ground state via disassociation into Kr and F while emitting a photon at 248 nm.

not in the ground state. The excimer molecule has a short upper-state lifetime, and it decays to the ground state through disassociation while emitting a photon.<sup>8</sup> There are two types of excimers: rare gas excited dimers, such as  $\text{Xe}_2^*$  and  $\text{Kr}_2^*$ , and the rare gas halogens, such as  $\text{XeF}^*$ ,  $\text{XeCl}^*$ ,  $\text{KrF}^*$ , and  $\text{ArF}^*$ . The latter class of excimers are of greater interest because they emit deep-UV photons (351, 308, 248, and 193 nm). The rare gas halogen excimer is generally pumped using a fast electrical discharge circuit. The gain lasts for a short time (20 to 30 ns), and as a consequence, there are only a few photon round trips through the gain medium. The output is highly multimode and spatially incoherent. This makes it suitable for lithography, because speckle problems are minimal. The excimer laser is essentially an amplifying flash lamp.

The following section presents the basic principles of excimer laser physics, system description, spectral narrowing, and wavelength diagnostics. Finally, we present the specifications of a production lithography laser in Sec. 3.

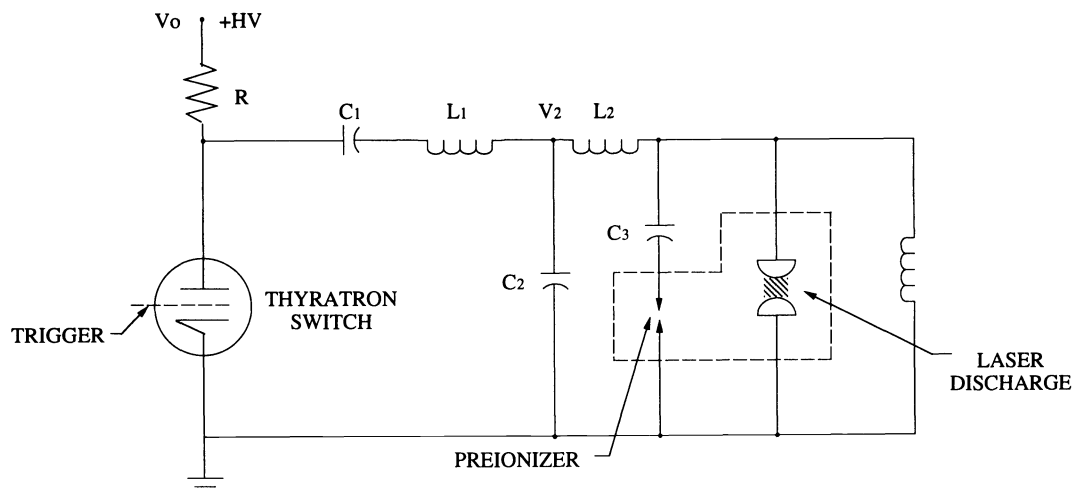
## 2.1 Operating Principles of Discharge Excimer Laser

All commercial excimer lasers use an electric discharge to excite and ionize the gas to create the upper state  $\text{KrF}^*$  molecule (Fig. 1). A typical electrical circuit used for this purpose is shown in Fig. 2. The operating sequence of this circuit is as follows:

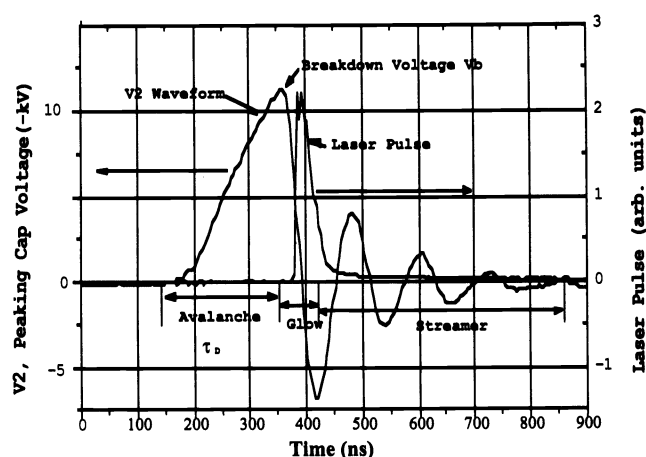
1. The HV supply charges the storage capacitor  $C_1$  (approximately 1.5 ms).
2. The thyatron is triggered to commute (or short).
3. The  $C_1$  pulse charges the peaking capacitors (approximately 180 ns).
4. As  $C_2$  charges, voltage appears between the electrodes.
5. When the voltage across  $C_2$  reaches a certain threshold, the gap between the electrodes breaks down and it conducts heavily.
6. If conditions are right, the discharge forms an amplifying gain medium and laser energy can be extracted.
7. Subsequently, any residual energy is dissipated in the discharge and in the electrodes.

Figure 3 shows the time evolution of the voltage on the peaking capacitors  $C_2$ , the discharge formations sequence, and the laser pulse. There are three distinct phases in the discharge process: avalanche, glow, and streamer.

The avalanche phase constitutes sequences 3 and 4 and is shown in Fig. 3. It lasts for approximately 180 ns, during which time preionization occurs. Preionization is essential to initiate the avalanche phase and is generally achieved through either arcs or coronas to generate very deep UV photons that ionize the gas to create an initial electron density of  $10^6$  to  $10^8$  per cubic centimeter. Avalanche proceeds by direct electron excitation of Kr to create  $\text{Kr}^+$  in a two-step ionization process:



**Fig. 2** Typical discharge circuit for excimer laser:  $C_1$ , inherent main storage capacitor;  $C_2$ , peaking capacitor;  $C_3$ , preionizer capacitor; and  $L_1$  and  $L_2$ , inherent circuit inductances. Preionizers are located on both sides of the discharge.



**Fig. 3** Three discharge phases—avalanche, glow, and streamer. The voltage  $V_2$  across the peaking capacitors  $C_2$  clearly delineates the three phases. The laser pulse appears during the glow (or the gain) phase.

However, avalanche is also moderated by loss of electrons through attachment with  $F_2$ :

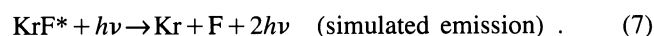
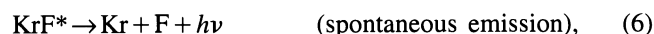


Subsequently, the electron density grows rapidly (exponentially), as a result of intense electrical fields in the vicinity of the discharge, until it reaches  $10^{13}$  per cubic centimeter. At this stage, voltage across the electrodes reaches a threshold and the next discharge phase, "glow," is initiated.

During the glow phase, energy from  $C_2$  is transferred to the region between the electrodes (sequence 5). This region conducts heavily and the upper state  $KrF^*$  excimer is formed via three-body reactions:



The excited  $KrF^*$  molecule decays to the ground level through dissociation into  $Kr$  and  $F$ . An amplifying gain medium is created by this dissociation with the emission of photons via both spontaneous and stimulated processes:

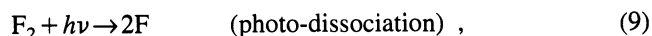


Laser energy is extracted, by means of an optical resonator, when the gain exceeds a certain threshold. The spectral bandwidth, full width at half maximum (FWHM) of a free running  $KrF$  excimer laser is approximately 300 pm. In the case of a lithography laser, spectral narrowing is achieved by feeding only a particular wavelength component of light back into the active gain region for amplification. The wavelength selection process takes place in the optical resonator by means of dispersive elements (see Sec. 2.3).

During the glow discharge phase, reformation of  $F_2$  begins through a three-body recombination reaction: a slow process that continues well beyond this phase:



The slow reformation of  $F_2$ , limits the formation of  $KrF^*$  [Eq. (4) and Eqs. (3) and (5)]; thus the short laser pulse duration. Increasing the  $F_2$  concentration, however, leads to other detrimental effects such as excessive loss of electrons due to attachment [Eq. (3)], leading to the collapse of the discharge into arcs. Increase in  $F_2$  also increases optical losses because of



As a consequence, for optimum discharge and gain conditions it is necessary to keep  $F_2$  and  $Kr$  concentration low in a high-pressure buffer gas such as neon. High pressure helps the formation of  $KrF^*$ , through three-body collisions [Eqs. (4) and (5)]. The nominal gas composition is 1%  $F_2$ , 1.2%  $Kr$ , and the balance  $Ne$  at a total pressure of 300 to 350 kPa.

Because of circuit inductances, impedance mismatch, and a short glow phase duration, not all the energy from  $C_2$  is transferred into the glow discharge phase. Residual energy is deposited into the next phase—"streamers." Energy lost in the streamer phase is a major contributor to electrode erosion and all its deleterious consequences.<sup>9</sup> These include the loss of fluorine because of continuous electrode passivation after each pulse, increase in discharge cross section, and the creation of metal fluoride dust. The streamer phase is detrimental, but is almost impossible to eliminate in any practical system.

The loss of fluorine is generally compensated by periodic injection of  $F_2$  into the discharge chamber. The increase in discharge cross section leads to increase in beam size and spectral bandwidth, and eventually to unacceptable performance. The metal fluoride dust created by electrode erosion is the cause for window contamination and increase in optical losses. This problem is solved by periodic cleaning of the windows along with the implementation of a dust trapping/window protection system. The metal fluoride dust is trapped by means of an electrostatic precipitator. A small amount of laser gas is extracted from the chamber and is passed over negatively charged high-field wires to trap the dust. The dust-free gas is then released over the windows to keep them clean. The gas is driven through the precipitator by the differential pressure built up inside the laser chamber because of the high velocity flow. In an efficient laser, the streamer phase can be minimized.

## 2.2 System Description

The excimer laser system for lithography consists of the following major modules:

1. laser chamber
2. pulse power module and HV power supply
3. optical resonator and the spectral narrowing module
4. wavemeter
5. control unit
6. peripheral support subsystems.

The laser system block diagram is shown schematically in Fig. 4. It shows the key modules except the peripheral support subsystems, such as the gas distribution module, the vacuum

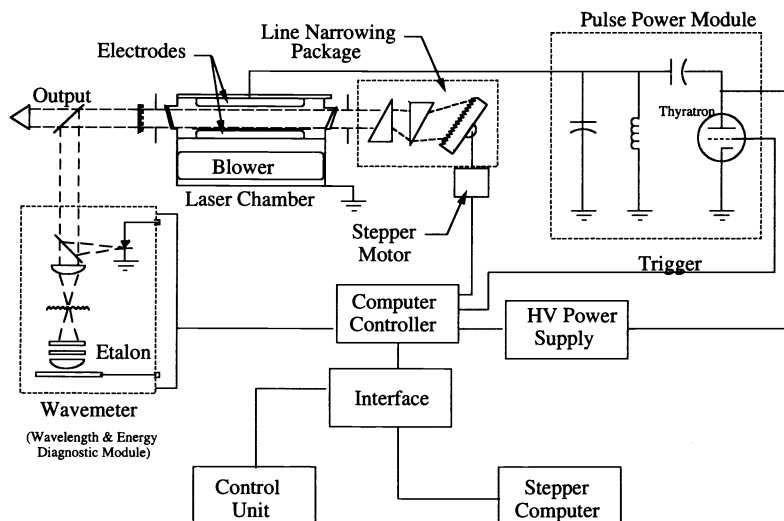


**Fig. 4** Lithography laser block diagram schematic showing major modules of the laser. The pulse power module and the chamber are very closely coupled in a real system.

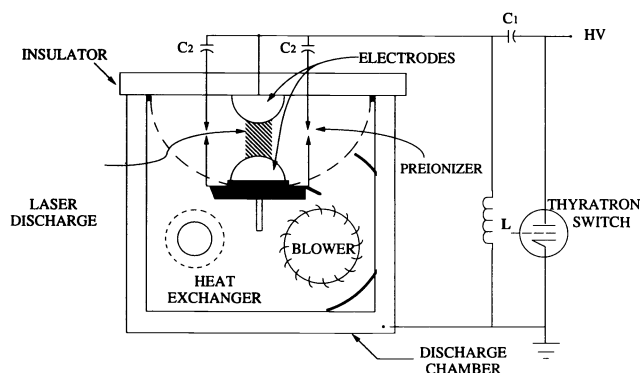


**Fig. 5** Schematic of a discharge excimer laser showing the location of the blower, electrodes, preionizer, and the heat exchanger.

pump out system, the electrical distribution, etc. Additional details of the laser chamber are shown in Fig. 5.

The pulse power module and the laser discharge chamber are physically closely coupled to minimize all stray inductance for fast energy transfer into the discharge. The discharge region ( $50 \times 1.6 \times 0.5 \text{ cm}^3$ ) is defined by the two electrodes separated by a gap of 1.6 cm. The cathode is supported by an insulating ceramic structure, whereas the anode is attached to the metal chamber. The preionization is done by corona (high voltage surface currents) structures located on either side of the discharge region. Because the laser is pulsed (400 to 500 Hz), it is essential to clear the discharge region between pulses—a task performed by a tangential blower, which is magnetically coupled to an external drive source. Heat is extracted from the laser gas by means of a water-cooled finned heat exchanger inside the chamber. Not shown in Fig. 5 is the metal fluoride dust trapping and window protection system. The use of noncontaminating and stable materials (such as ceramics and metals) is critical for improving the overall performance and reducing the laser operating cost.

Excimer lasers generally use organic materials such as Kynar or Teflon as electrical insulators, and viton elastomers

for o-ring gas seals.<sup>10</sup> All these materials contaminate the laser gas. This is particularly true in the presence of electrical discharge, fluorine, and ionic fluorine. As a consequence, gaseous contaminants such as  $\text{CF}_2$ ,  $\text{CF}_4$ ,  $\text{COF}_2$ ,  $\text{SiF}_4$ ,  $\text{CO}_2$ ,  $\text{HF}$ , and  $\text{SF}_6$  are pervasive in laser chambers that use such organic materials. These contaminants have several detrimental effects; they (1) absorb photons at 248 nm and thus reduce efficiency, (2) contaminate and etch windows, (3) decrease gas life, and (4) increase electrode erosion. To overcome this problem, most excimer lasers employ a cryogenic gas reprocessor to remove the gaseous contaminants. However, not all contamination can be removed in this manner.

The use of ceramics, metal o-rings, and pure metals (free of carbon, silicon or sulfur) for electrodes eliminate such gaseous contaminants. Excimer lasers (Sec. 3) based on such technologies are now available. These do not use a cryogenic gas reprocessor and are able to achieve extremely long gas (greater than 25 million pulses) and electrode life (greater than 2000 million pulses).

The pulse power module consists of a low-inductance storage capacitor, thyatron, ceramic peaking capacitors, thyatron support and trigger circuit, and a well-regulated switching-type high-voltage power supply. A thyatron is a hot cathode, deuterium filled, high-voltage shorting switch. It is capable of switching high currents (approximately 15 kA) in a short duration (30 ns) at high repetition rates. The thyatron is a well-engineered switch, and was developed initially for radar applications. It is now also used for switching excimer lasers. The newest generation of thyatrons have excellent performance in terms of low prefires (less than 1 in  $10^7$  pulses) and a long operating life (greater than  $2 \times 10^7$  pulses) [English electric valve (EEV), CX-1625].

### 2.3 Spectral Narrowing of a KrF Laser

The bandwidth (FWHM) of a free running KrF excimer laser is approximately 300 pm. As discussed earlier, an excimer stepper requires the output of the laser to be spectrally narrowed between 1 and 3 pm depending on the NA of the lens.

Spectral narrowing of an excimer laser can be accomplished in several ways. It is based on introducing wavelength

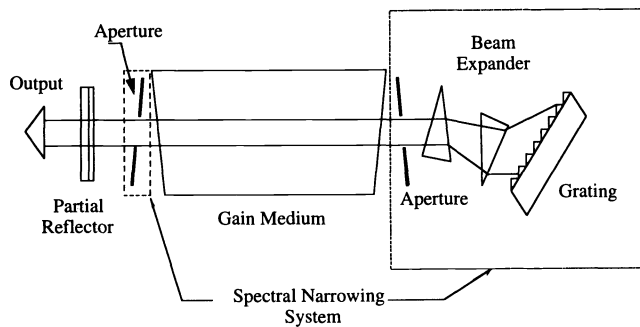


**Fig. 6** Spectral narrowing of a KrF excimer laser using a grating in Littrow configuration. The prisms are used to expand the beam; the aperture controls the bandwidth.

dispersive optical elements in the resonator. Three types of dispersive elements can be used: prisms, etalons, and gratings. Prisms do not provide enough dispersion and are thus unsuitable. Etalons are highly dispersive and efficient for spectrally narrowing an excimer laser.<sup>11</sup> In fact, many of the earlier lithography excimer lasers used a pair of etalons for spectral narrowing. However, etalons suffer from two major shortcomings: thermal drift and coating damage. Both of these problems limit the use of etalons in a conventional optical setup for spectral narrowing. This problem was, however, solved by placing the etalons in a secondary optical branch in a novel polarization-coupled resonator (PCR) configuration.<sup>12</sup> But this system is fairly complex and difficult to implement.

The use of a high dispersive grating in a Littrow configuration is the simplest and most effective spectral-line-narrowing technique (Fig. 6). Three prisms are used to expand the beam by a factor of approximately 15 before it is incident on the grating. The illuminated area on the grating is roughly  $12 \times 1.6$  cm. The diffracted light that is returned in the same direction as the incident beam (Littrow configuration) is amplified by the gain medium. The use of a large grating, in addition to offering high dispersion, results in reduced thermal and optical loading, hence a more thermally stable and long lasting spectral narrowing unit. Two apertures, one on each end of the gain medium are used to select the spectral bandwidth. The resulting bandwidth is a function of grating dispersive power, grating area exposed, slit widths, and the number of optical round trips. Similarly, other grating-based spectral narrowing schemes can be employed, such as using a second mirror to use the grating surface twice for achieving higher dispersion.<sup>11</sup> However, the scheme discussed here is more compact. Wavelength tuning is accomplished by changing the angle of incidence of light on the grating.

Because the need for narrower and narrower spectral bandwidth increases for higher NA lenses, the optical quality of the dispersive elements for spectral narrowing has to improve accordingly. Small deviations from flatness or material homogeneity causes wave front errors and spectral broadening. The KrF gain medium amplifies these errors, which results in an increase in bandwidth. The selection of defect-free optics, therefore, becomes critical. However, the problem of minor wave front curvature (which causes increase in bandwidth) can be solved in a novel way by introducing a small (concave or convex) curvature in the grating.<sup>13</sup> This is ac-

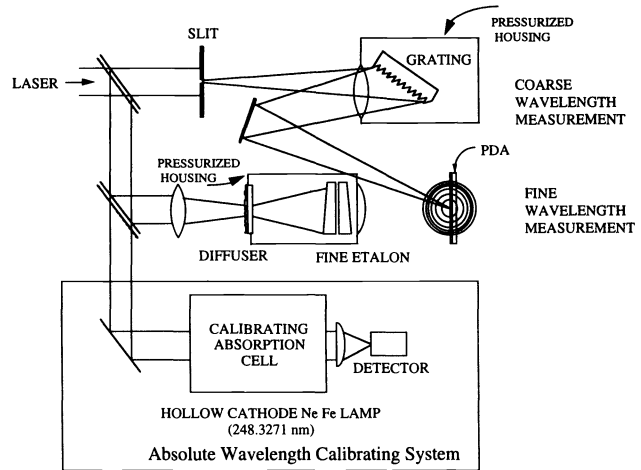


**Fig. 7** Wave meter based on etalon and grating. The grating is used for coarse measurement, whereas the etalon does the fine measurement. Absolute wavelength calibration is done off-line in the factory.

complished by physically bending the grating by means of a clamp and screw arrangement. The radius of curvature thus introduced to the grating could be between 0.5 and 10 km. This method allows one to achieve very narrow spectral bandwidths (less than 1 pm) with good efficiency.

## 2.4 Wavelength and Bandwidth Measurement

The center wavelength of the lithography laser output radiation has to be stabilized in order to (1) maintain focus at the wafer plane and (2) minimize any change in magnification. Drift in center wavelength, however, affects the focal plane stability more severely than magnification. In this section, we discuss the technique used to measure and stabilize the laser center wavelength.

The "wave meter" used for a production lithography laser has to be compact and yet meet the requirements of good relative accuracy, small long-term drift, and a good absolute precision with reference to an atomic line. The requirement in each case is less than  $\pm 0.15$  pm. Further, the wavelength measurement has to be insensitive to changes in the ambient temperature or pressure. In addition, the wave meter should be capable of measuring the spectral bandwidth (FWHM) with an accuracy of  $\pm 0.15$  pm. The operating range of this wave meter, on the other hand, can be relatively small,  $248.35 \pm 0.30$  nm.

In the lithography laser discussed in Sec. 3, the wavelength is measured using a combination of a grating and an etalon. A schematic layout of this wave meter is shown<sup>14</sup> in Fig. 7. The grating and the etalons are used respectively for coarse and fine measurements. The output from the grating spectrometer is imaged in the central region of a 1024 element silicon photodiode array, whereas the fringe pattern from the etalon is imaged on the two sides (Fig. 8). Note the central image from the etalon is blocked. The wavelength is determined by measuring the diameter of the etalon fringe pattern and the position of the coarse grating output.

Wavelength stabilization based on measuring the diameters of etalon fringe pattern is well established.<sup>15</sup> This scheme is insensitive to mechanical alignment errors and

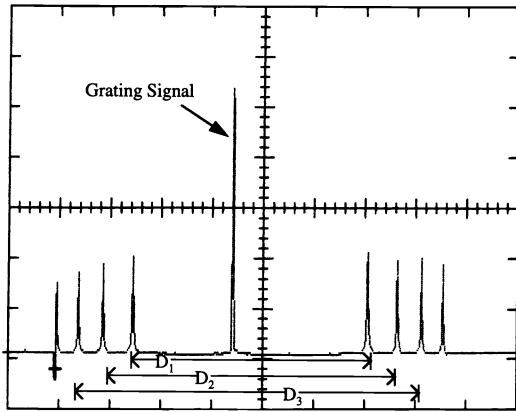


**Fig. 8** Wave meter full fringe pattern. The central fringe is the coarse grating signal and the outer peaks on both sides are the fine etalon fringes. Diameters  $D_1$ ,  $D_2$ , and  $D_3$  of the etalon fringes are used to determine laser wavelength.

small changes in input beam directions. The diameter  $D_{pr}$  of the  $p$  interference fringe from the center of the fringe pattern is given by

$$D_{pr}^2 = 4f^2\lambda_r(p - 1 + \epsilon_r)/(\mu_r h), \quad p = 1, 2, \dots, \quad (11)$$

where  $\mu_r$  is the refractive index of the intraetalon medium at the wavelength  $\lambda_r$ ,  $\epsilon_r$  ( $0 \leq \epsilon_r \leq 1$ ) is the fractional order number at the center of the fringe pattern,  $f$  is the focal length of the imaging lens, and  $h$  is the etalon mirror spacing. As can be seen from Eq. (11), a small change in fringe diameter is proportional to change in the wavelength. For wavelength change less than the free spectral range (FSR) of the etalon, the etalon is capable of tracking the wavelength of the laser. The coarse grating measurement is necessary to eliminate any possible error or discrepancy in the laser wavelength drift of greater than the FSR of the etalon (20 pm). As is well known, the etalon fringe pattern is identical for wavelengths separated by multiples of its FSR.

In this wave meter, the resolution of the grating measurement is  $\pm 0.5$  pm, while its long-term accuracy is  $\pm 0.5$  pm. The etalon, on the other hand, has a resolution of  $\pm 0.1$  pm and long-term accuracy of  $\pm 0.25$  pm.

Figure 8 shows both the coarse and fine fringe patterns. The full pattern is used to determine the laser wavelength. The wave meter is calibrated at the factory with reference to a hollow cathode Ne-Fe lamp that has an absorption peak at 248.3271 nm. Therefore, the wave meter on the laser does not have a built-in absolute reference source for calibration. The present wave meter has exhibited, over the years and in the field, an excellent long-term absolute measurement stability (less than  $\pm 0.5$  pm). Furthermore, to eliminate ambient pressure-dependent changes, both the grating and the etalon are housed inside individual pressurized housings, see Fig. 7. Temperature stability is achieved by using very low thermal expansion coefficient etalon spacers and good thermal management of the etalon housing.

The bandwidth of the laser output is measured from the etalon fringe pattern. Note that the separation between neighboring fringes is one FSR, 20 pm (Fig. 9). Consequently, a fringe nestled between two other fringes provides a scale to measure the laser bandwidth directly from the fringe band-

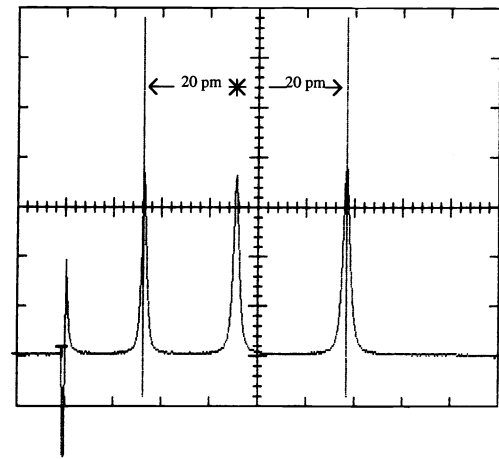


**Fig. 9** Fine etalon fringe pattern—one side. These are used to determine spectral bandwidth (FWHM). Note the separation between the fringes is 20 pm (FSR).

width. This pattern is used to determine the spectral bandwidth of the laser. If the etalon used has a finesse ( $F = 30$ ), then the etalon resolution or bandwidth is  $\text{FSR}/F = 0.67$  pm. Therefore, the measurement of the spectral bandwidth (FWHM) from the etalon fringe pattern width is not strictly correct; the fringe measurement has to be deconvolved for the etalon bandwidth.<sup>16</sup> In addition, the fringe pattern does not provide a good idea of the spectral energy content in the wings. For this, one has to use a high-resolution spectrometer.<sup>17</sup> In any event, the etalon fringe pattern does provide a good reference to track changes in the laser spectral bandwidth.

Finally, the wavelength information obtained from the wave meter is used to control laser wavelength by changing the angle of illumination on the grating in the line narrowing module (Fig. 7). The bandwidth of the laser, which is controlled by the aperture size, can not be changed in the field.

### 3 Performance Specifications and Maintenance Issues of a Lithography Laser, Model ELS-4000D

The performance specifications for a lithography laser are determined by the requirements of the stepper, resist, characteristics, and throughput issues. As seen in Table 1, as the stepper performance has progressed, the requirements on the laser have become more stringent. The latest stepper models suitable for sub-0.4- $\mu\text{m}$  resolution in production, are equipped with a variable NA lens (0.35 to more than 0.5), variable coherence  $\sigma$  illuminator (0.3 to 0.7), and a large exposure field capability (greater than  $21 \times 21$  mm<sup>2</sup>). Furthermore, several process worthy, modest cost, deep-UV positive tone resists, with a sensitivity between 30 and 60 mJ/cm<sup>2</sup> are now commercially available. The excimer laser common to all these stepper models is the Cymer laser, series ELS-4000. Performance specifications for the latest model laser (ELS-4000D) are given in Table 3. A detailed system configuration and layout of this laser is shown in Fig. 10. The laser was designed for use in an actual IC fab line. It features a highly modular system layout for easy and fast service. In addition, it meets all operational and semiconductor industry safety codes.

**Table 3** ELS-4000D performance specifications.

Center Wavelength	248.35 nm
Wavelength Tuning Range	$\pm 150$ pm
Repetition Rate	500 Hz
Pulse Energy	12 mJ
Power	6 W
Spectral Bandwidth (FWHM)	$\leq 1.3$ pm
Band for 95% Energy	$< 4$ pm
Pulse-to-Pulse Energy Variations ( $1\sigma$ )	$< 2.5\%$
Wavelength Drift Over 8 Hours	$\leq \pm 0.25$ pm
Wavelength Drift Over 6 Months	$\leq \pm 0.25$ pm

The ELS-4000D is a 6-W (12 mJ at 500 Hz), spectrally narrowed (less than or equal to 1.3 pm) laser. Figures 11 and 12 show the spectral profile and the integrated energy distribution, respectively. These were measured on a high-resolution (0.2-pm) grating spectrometer.<sup>17</sup> It should be noted that the integrated energy spectrum, and the spectral width for 95% energy are more critical to stepper performance than just the FWHM value. The wavelength stability during an exposure (burst) mode is shown in Fig. 13, and the pulse energy stability is exhibited in Fig. 14. The spatial coherence properties of the laser output are shown in Fig. 15. The vertical and horizontal coherence lengths<sup>16</sup> are, respectively, 92 and 187  $\mu\text{m}$ .

#### Laser Maintenance

Like any other equipment, the excimer laser requires periodic servicing. Unlike mercury lamps, which are discarded after a certain number of usage hours, laser maintenance is based on refurbishing and reusing modules after fairly long, but regular, intervals.

Presently, lithography excimer lasers in the field require low maintenance (both scheduled and unscheduled) and have demonstrated good production worthiness. However, continuous progress is being made to extend maintenance intervals and lifetime of modules in an attempt to lower laser operating cost to a level comparable to the use of *i*-line mercury lamps. Before we discuss maintenance schedules, it is useful to estimate the laser usage during actual production. Note that unlike a mercury lamp, the laser is operating only during exposure. The model used to estimate laser usage is based on a resist sensitivity of 50 mJ/cm<sup>2</sup> and an optical throughput efficiency of 16%, both fairly typical values. As a result, laser usage during production will be approximately  $2 \times 10^9$  pulses (Table 4) in 1 yr.

Scheduled maintenance intervals for the ELS-4000D, based on extensive in-house tests and detailed characterization, are given in Table 5. Note that except for gas exchange and fluorine trap replacement, other action items call for checking performance before proceeding to replace the part of the module. The intervals shown here are for reference. For higher stepper uptime and availability, laser maintenance will generally be synchronized to coincide with scheduled stepper maintenance. The operating cost for the laser today is approximately \$20,000 for 1000 million pulses and is expected to decrease by an additional 20 to 30% in the future. It will then compare favorably with the use of a high-intensity mercury lamp in an advanced *i*-line stepper. The reliability of the laser, in terms of mean time between failures (MTBF), now exceeds 3000 h, whereas the uptime or availability of a properly maintained laser is better than 95%.

#### 4 Summary and Outlook

The krypton fluoride excimer laser for lithography, after a difficult beginning, is now a production worthy, fab-line-qualified manufacturing tool. It is now able to meet all the stepper and process requirements in terms of performance, reliability, and operating costs. Improvements in system design and engineering were responsible for this.

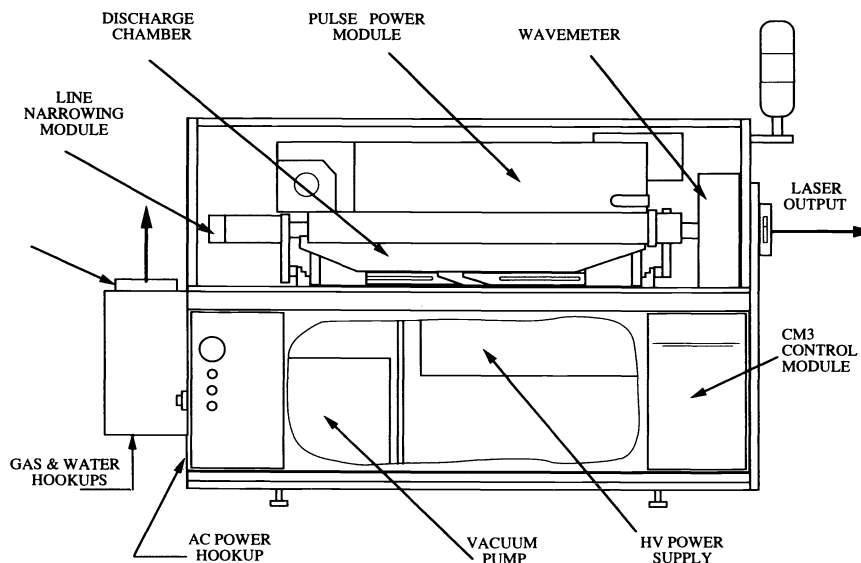


**Fig. 10** ELS-4000 system layout. All modules are easily accessible for fast replacement to minimize downtime. The chamber can be rolled out (without disturbing optical alignment) for window maintenance.



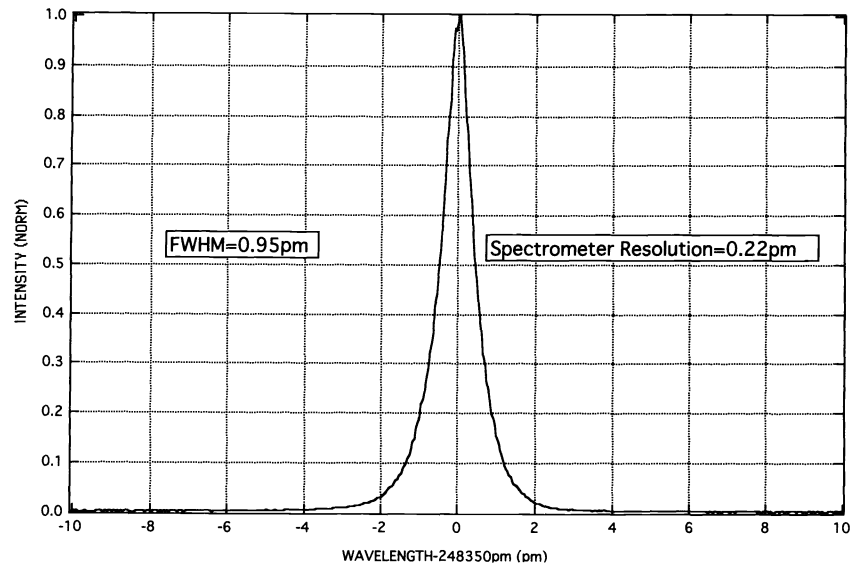


**Fig. 11** Laser spectrum narrowed on high-resolution (0.22-pm) grating spectrometer. The undeconvolved bandwidth (full width at half maximum) is 0.95 pm.

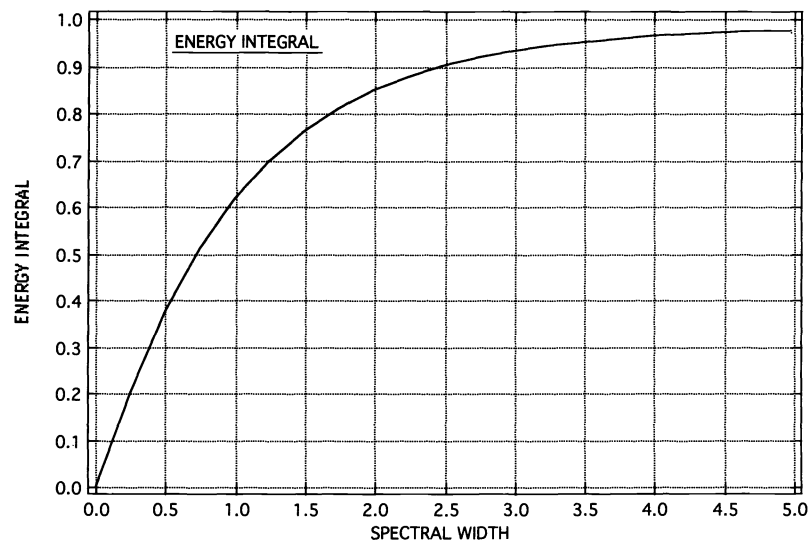


**Fig. 12** Spectral energy integral measured on high-resolution grating spectrometer. Note that 95% of integrated spectral energy is within 3.5 pm.

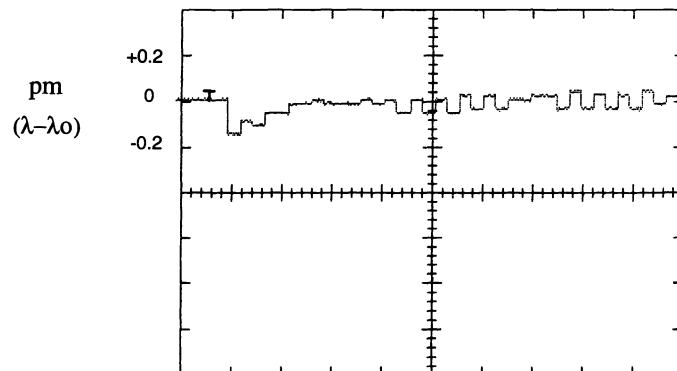


**Fig. 13** Central wavelength drift during an exposure. Note that the first pulse shows a wavelength chirp of  $-0.2$  pm.

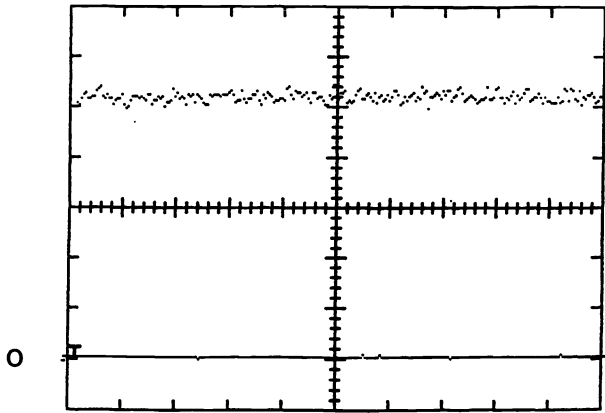


**Fig. 14** Pulse-to-pulse energy stability for an exposure. The voltage has been adjusted to minimize energy spiking during the initial phase:  $1\sigma = 2.3\%$ .

Lithography needs for sub-0.4- $\mu\text{m}$  resolution, such as 64 M DRAM and 16 M static random access memory, will be met by *i*-line and excimer steppers. The excimer stepper will be used for some critical layers. The next generation of KrF excimer steppers for sub-0.3- $\mu\text{m}$  resolution, will employ lenses with  $\text{NA} > 0.6$  and a field size exceeding  $21 \times 21 \text{ mm}^2$ . The laser for this will require a spectral bandwidth of less than 0.8 pm (FWHM) with an output power of 6 to 8 W. We foresee no difficulty in meeting these specifications. Following krypton fluoride, argon fluoride (193-nm) excimer lithography is expected to push the limits of optical lithography below 0.25- $\mu\text{m}$  resolution.

Finally, the operating cost of the laser is now comparable to the use of *i*-line mercury lamps. Uptime and availability is, however, higher.

#### Acknowledgments

The author would like to thank Dr. P. Das, Dr. R. Sandstrom, Dr. I. Fomenkov, and Dr. T. Ishihara for technical discussions and ideas in the preparation of this paper.

**Table 4** Estimated laser usage during production.

Resist Sensitivity	50 mJ / $\text{cm}^2$
Field Size	22 x 22 $\text{mm}^2$
Laser Power	6 W
Repetition Rate	500 Hz
Power At Wafer	200 mW/ $\text{cm}^2$
Exposure Time	0.25 seconds
Number of Pulses / Exposure	120
Wafer Size	200 mm
Die Sites / Wafer	60
Throughput	45 W / Hr.
Laser Pulse per Hour	$3.24 \times 10^5$
Average Utilization (over 1 year [8670 hrs.])	60%
Pulses per Year	$1.7 \times 10^9$

#### References

1. M. Bigelow, J. Greeneich, and P. Jenkin, "Optical strategies for achieving  $\sim 0.25 \mu\text{m}$  design rules," *Microlithogr. World* **2**, 9-14 (1993).
2. A. V. Hill, J. E. Webb, A. R. Phillips, and J. E. Connors, "Design and analysis of a high NA projection optical system for 0.35  $\mu\text{m}$  deep-UV lithography," in *Optical/Laser Microlithography VI, Proc. SPIE* **1927**, 608-621 (1993).
3. S. Wittekoek, M. A. van den Brink, G. Poppelaars, M. Reuhman-Huiskens, A. Grassmann, and U. Boettger, "Wide field deep-UV wafer stepper for 0.35 micron production," in *Optical/Laser Microlithography VI, Proc. SPIE* **1927**, 582-594 (1993).
4. G. Escher, G. Telpot, and R. Mohdro, "Advances in deep-UV resist processing," in *Advances in Resist Technology and Processing X, Proc. SPIE* **1925** (1993).
5. W. Brunsvold, K. Stewart, P. Jagannathan, J. Parrill, R. Sooriyakumaran, P. Muller, and H. Sachdev, "Evaluation of a deep-UV bilayer resist for 64 Mb DRAM production," in *Advances in Resist Technology and Processing X, Microlithography VI, Proc. SPIE* **1925** (1993).
6. P. Leuermann, P. van Oorschot, H. Jasper, S. Stalnaker, S. Brainerd, B. Rolfson, and L. Karklin, "0.35 micron lithography using off-axis illumination," in *Optical/Laser Microlithography, Proc. SPIE* **1927**, 103-124 (1993).
7. Model ELS-4000 Excimer Laser, Cymer Laser Technologies. For a description of this laser please refer to T. Ishihara, R. Sandstrom, C. Reiser, and U. Sengupta, "Advanced krypton fluoride excimer laser

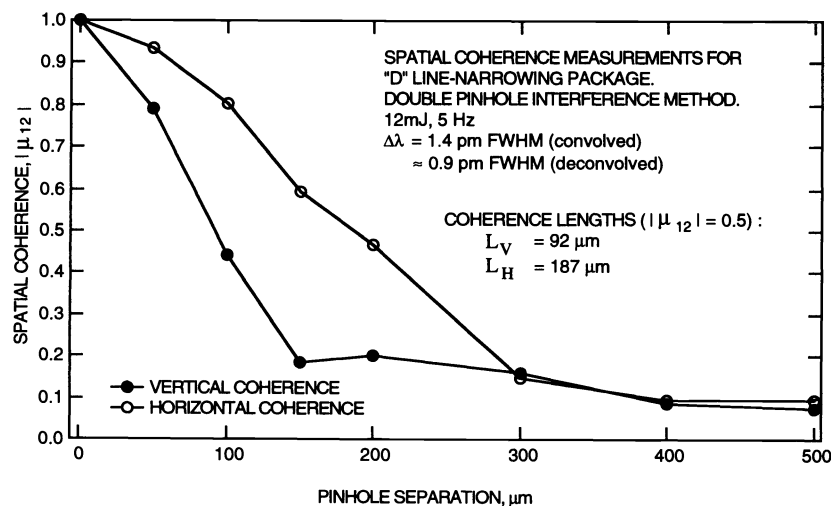


**Fig. 15** Spatial coherence measured using a pair of pin holes at various separations.

**Table 5** Maintenance schedule.

ACTIVITY	INTERVAL IN PULSES
Gas Exchange	25 M or 3 days
Fluorine Trap	250 Refills
Window Inspection / Clean <sup>1</sup>	> 500 M
Optics Inspection / Exchange <sup>1</sup>	> 1000 M
Inspect, Recalibrate & Qualify Laser <sup>1</sup>	> 1000 M
Laser Chamber (min.) <sup>2</sup>	> 2000 M
Line Narrowing Module (min.) <sup>2</sup>	> 3000 M

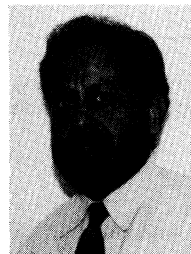
<sup>1</sup> Check baseline performance: voltage versus energy, bandwidth. Recalibrate if necessary.

<sup>2</sup> (a) Check baseline performance: voltage versus energy, bandwidth, and pulse energy stability, and (b) phototest: resolution versus DOF.

for microlithography," in *Optical/Laser Microlithography V, Proc. SPIE 1674*, 473-485 (1992).

8. Ch. K. Rhodes, Ed., *Topics in Applied Physics*, Vol. 30, *Excimer Lasers*, Springer-Verlag (1979).
9. U. Sengupta, T. Ishihara, and R. Sandstrom, "Parametric studies and the operating latitude of a spectrally narrowed KrF excimer laser for the deep-UV stepper," in *Optical/Laser Microlithography XI, Proc. SPIE 1927*, 252-262 (1993).
10. DuPont trademark materials.
11. T. J. Mckee, "Spectral-narrowing techniques for excimer laser oscillators," *Can. J. Phys.* **63**, 214-219 (1985).
12. N. Furuya, T. Ono, N. Horiuchi, K. Yamanaka, and T. Miyata, "High power and narrow band excimer laser with a polarization coupled resonator," in *Optical/Laser Microlithography III, Proc. SPIE 1264*, 520-531 (1990).

13. R. Sandstrom, "Spectral narrowing technique," U.S. Patent No. 5,095,492 (1992).
14. R. Sandstrom and S. Anderson, "System for, and method of, regulating the wavelength of a light beam," U.S. Patent No. 5,025,445 (1991).
15. K. Dasgupta and R. Srivastava, "Wavelength stabilization and control of pulses or CW tunable dye lasers: a simple scheme," *Appl. Opt.* **26**, 3659-3662 (1987).
16. R. Sandstrom, "Measurements of beam characteristics relevant to DUV microlithography on a KrF excimer laser," in *Optical/Laser Microlithography III, Proc. SPIE 1264*, 505-519 (1990).
17. I. V. Fomenkov and R. Sandstrom, "High resolution spectral studies and the absolute wavelength calibration of a KrF excimer laser for microlithography," in *Optical/Laser Microlithography XI, Proc. SPIE 1927*, 744-751 (1993).



**Uday K. Sengupta** received a BS (1968) and a PhD (1974) in electrical engineering/mathematics from Ohio State University, Columbus. He has worked in R&D at Tachisto, Needham, Massachusetts, and has been a senior research scientist and commercial marketing manager at HLX, Inc. He was a founding member and staff scientist at Lasertechnics and was instrumental in positioning Lasertechnics in the laser marketing market. He cofounded and serves as the vice-president of marketing at Cymer Laser Technologies and stays actively involved in the development and refinement of Cymer's lasers.